



Alkali and alkaline-earth metal dodecahydro-*closo*-dodecaborates: Probing structural variations *via* neutron vibrational spectroscopy

Nina Verdal^{a,*}, Wei Zhou^{a,b}, Vitalie Stavila^c, Jae-Hyuk Her^{a,b,1}, Muhammed Yousufuddin^{a,b,2}, Taner Yildirim^{a,d}, Terrence J. Udovic^a

^a NIST Center for Neutron Research, National Institute of Standards and Technology, 100 Bureau Dr., MS 6102, Gaithersburg, MD 20899-6102, United States

^b Department of Materials Science and Engineering, University of Maryland, College Park, MD 20742, United States

^c Sandia National Laboratories, 7011 East Avenue, Livermore, CA 94551-0969, United States

^d Department of Materials Science and Engineering, University of Pennsylvania, Philadelphia, PA 19104, United States

ARTICLE INFO

Article history:

Received 16 July 2010

Accepted 7 August 2010

Available online 17 August 2010

Keywords:

Boron hydride

Density functional theory

Dodecahydro-*closo*-dodecaborate

Neutron vibrational spectroscopy

Phonon density of states

First principles calculations

ABSTRACT

The hydrogen-weighted phonon densities of states for the series of alkali (A = Li, Na, K, Rb, and Cs) and alkaline-earth (Ae = Mg, Ca, Sr, and Ba) metal dodecahydro-*closo*-dodecaborates, $A_2B_{12}H_{12}$ and $AeB_{12}H_{12}$, were measured *via* neutron vibrational spectroscopy (NVS). Using the known crystal structures, density functional theory (DFT) phonon calculations were able to closely replicate the observed vibrational spectra. The spectral details were found to differ considerably with structure, indicating that the internal vibrations of the $B_{12}H_{12}^{2-}$ icosahedral anions are sensitive to symmetry-dependent interactions with their crystal surroundings. In contrast, these internal vibrations were relatively unchanged among isomorphous $A_2B_{12}H_{12}$ and $AeB_{12}H_{12}$ compounds possessing different metal cations. These results confirm that the combination of NVS and DFT phonon calculations can be used to help validate postulated local crystal symmetries in these types of materials, even in instances where the ordering is only short-range, rendering the materials amorphous with respect to diffraction probes.

Published by Elsevier B.V.

1. Introduction

Alkali (A = Li, Na, K, Rb, and Cs) and alkaline-earth (Ae = Mg, Ca, Sr, and Ba) metal dodecahydro-*closo*-dodecaborates, $A_2B_{12}H_{12}$ and $AeB_{12}H_{12}$, are of current interest in hydrogen-storage research as they are possible intermediates [1–7] in the dehydrogenation of the related borohydrides ABH_4 and $Ae(BH_4)_2$. They have been detected as an amorphous component of dehydrogenation products using NMR spectroscopy [1] and their presence was confirmed in subsequent studies [6–8]. Any $B_{12}H_{12}^{2-}$ anions produced during dehydrogenation are likely resistant to rehydrogenation: *e.g.*, under aggressive rehydrogenation conditions (100 MPa H_2 , 670 °C) a ball-milled mixture of $(CaB_{12}H_{12} + 5CaH_2)$ was not observed to convert to $Ca(BH_4)_2$ [9]. It is a concern that the creation of the stable dodecahydro-*closo*-dodecaborate intermediate under commonly used dehydrogenation conditions is partly responsible for the poor hydrogen cycling performance of the borohydrides [3,6,7,10]. To

aid in understanding the role of this intermediate, a more detailed knowledge of its vibrational spectroscopic signature is highly desirable.

The vibrational spectra of dodecahydro-*closo*-dodecaborates in the solid state differ considerably from that of the isolated dianion, even in solution [11]. Allis and Hudson [12] reported that the solid-state vibrational spectrum of $Cs_2B_{12}H_{12}$ could not be reproduced with an isolated-ion calculation, but found good agreement using a solid-state calculation. The source of the differences between the solid-state and isolated-molecule spectra is thought to stem from a change in the symmetry of the icosahedron with crystal packing. Due to the relatively large neutron scattering cross-section for hydrogen, the features in a neutron vibrational spectrum result primarily from hydrogen atom displacements, with only very minor contributions from the much more weakly scattering elements. In this paper, we show that the neutron vibrational spectra for all alkali and alkaline-earth metal dodecahydro-*closo*-dodecaborates are sensitive to the crystalline environment and the space group symmetry, and these spectra can be successfully reproduced by solid-state DFT calculations.

Typically, the dodecahydro-*closo*-dodecaborates that form during borohydride dehydrogenation do not crystallize with long-range order [1–5], but most likely exist as short-range-ordered arrangements of anions and cations that appear amorphous in a diffraction measurement. We demonstrate here that, since NVS is

* Corresponding author.

E-mail address: nina.verdal@nist.gov (N. Verdal).

¹ Current address: GE Global Research, 1 Research Circle, Niskayuna, NY 12309, United States.

² Current address: Department of Chemistry and Biochemistry, University of Texas at Arlington, Arlington, TX 76019, United States.

a much more local probe than diffraction, it can potentially be used to characterize these intermediates even when diffraction is not a suitable option.

2. Experimental details

Aqueous solutions of alkali and alkaline-earth dodecahydro-closo-dodecaborates were prepared by a solution route employing $[\text{H}_3\text{O}^+]_2[\text{B}_{12}\text{H}_{12}^{2-}]$ and the corresponding metal carbonates or hydroxides. Hydrates of various compositions were obtained upon the removal of water. Non-aqueous $\text{MgB}_{12}\text{H}_{12}$ was obtained by reacting $\text{Mg}(\text{BH}_4)_2$ and $\text{B}_{10}\text{H}_{14}$ in tetrahydrofuran (THF) at reflux. Solvent-free alkali and alkaline-earth dodecahydro-closo-dodecaborates were synthesized by heating the as-prepared solvates in vacuum between 200 °C and 350 °C. Unfortunately, the final $\text{MgB}_{12}\text{H}_{12}$ sample still possessed 0.5 THF molecules/ $\text{B}_{12}\text{H}_{12}^{2-}$ anion as determined by neutron prompt-gamma activation analysis. The $\text{Cs}_2\text{B}_{12}\text{H}_{12}$, $\text{BaB}_{12}\text{H}_{12}$, and $\text{Rb}_2\text{B}_{12}\text{H}_{12}$ presented in this work are ^{11}B labeled, using purchased $\text{Cs}_2^{11}\text{B}_{12}\text{H}_{12}$ (>98% chemical purity, 99.5% isotopic purity) as the starting material. Eliminating the highly absorbing ^{10}B isotope from the sample increases the neutron scattering intensity and data quality considerably.

NVS data were collected at 4 K using the BT4 Filter Analyzer Neutron Spectrometer [13] at the NIST Center for Neutron Research. The powder samples were placed inside an aluminum cell that was then loaded into a closed-cycle refrigerator. A $\text{Cu}(220)$ monochromator was used with pre- and post-monochromator collimations of 20 min of arc.

3. Theoretical calculations

First principles calculations were performed within the plane-wave implementation of density functional theory (DFT) using the PWscf package [14]. We used Vanderbilt-type ultrasoft potentials with Perdew–Burke–Ernzerhof exchange correlation. A cutoff energy of 544 eV was found to be enough for the total energy to converge within 0.5 meV/atom. Structure optimizations were first performed with respect to atomic positions, with the lattice parameters fixed at the experimental values. Phonon calculations were then performed on the relaxed structures using the supercell method with finite displacements [15]. For the isolated $\text{B}_{12}\text{H}_{12}^{2-}$ anion, a $30 \times 30 \times 30$ supercell was used, and its full I_h molecular symmetry was considered in the phonon calculation.

4. Results and discussion

Neutron vibrational spectra were collected for the alkali metal dodecahydro-closo-dodecaborates $\text{Li}_2\text{B}_{12}\text{H}_{12}$, $\text{Na}_2\text{B}_{12}\text{H}_{12}$, $\text{K}_2\text{B}_{12}\text{H}_{12}$, $\text{Rb}_2^{11}\text{B}_{12}\text{H}_{12}$ and $\text{Cs}_2^{11}\text{B}_{12}\text{H}_{12}$ and for the alkaline-earth metal dodecahydro-closo-dodecaborates $\text{MgB}_{12}\text{H}_{12}$ (partially solvated), $\text{CaB}_{12}\text{H}_{12}$, $\text{SrB}_{12}\text{H}_{12}$, and $\text{Ba}^{11}\text{B}_{12}\text{H}_{12}$. These spectra were compared with the simulated phonon densities of states determined from the DFT-optimized crystal geometry, weighted appropriately for the atomic neutron scattering cross-sections of the different atoms and broadened according to the spectrometer resolution. All DFT phonon calculations assume a boron mass based on the natural abundance of its isotopes. Therefore, the observed spectra for the samples of $\text{Rb}_2^{11}\text{B}_{12}\text{H}_{12}$, $\text{Cs}_2^{11}\text{B}_{12}\text{H}_{12}$, and $\text{Ba}^{11}\text{B}_{12}\text{H}_{12}$ are expected to be slightly downshifted from the calculation, and in general exhibit sharper peaks than their natural abundance counterparts.

Neutron vibrational spectra are shown in Fig. 1 for both crystalline and amorphous $\text{Li}_2\text{B}_{12}\text{H}_{12}$ (as determined by X-ray diffraction (XRD)), the latter formed by dehydration in air at ~200 °C. In general, observed spectral features in this region represent the optical vibrational modes of the $\text{B}_{12}\text{H}_{12}^{2-}$ icosahedral cages, ranging from cage deformations and breathing modes at 65–100 meV, hydrogen wagging modes between 100 meV and 120 meV, and modes containing both hydrogen wags and cage deformations between 120 meV and 135 meV. The higher energy B–H stretching modes are not observed in these spectra. Although the spectrum of the amorphous sample exhibits slightly broadened features relative to the crystalline sample, which is consistent with

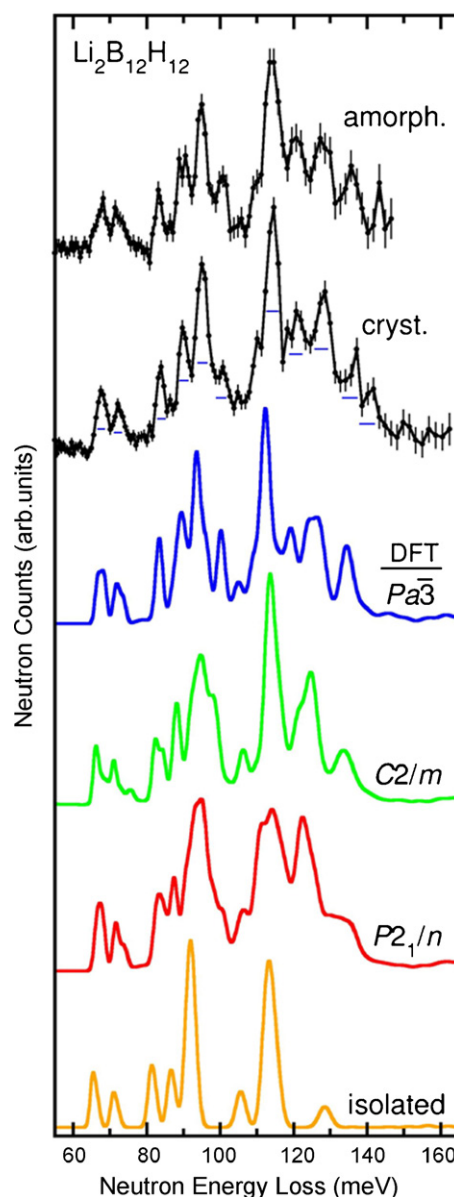


Fig. 1. $\text{Li}_2\text{B}_{12}\text{H}_{12}$ NVS spectra. Neutron vibrational spectra of (top to bottom): amorphous and crystalline (determined using XRD) $\text{Li}_2\text{B}_{12}\text{H}_{12}$, compared with simulated spectra using the experimentally determined [16] space group $\text{Pa}\bar{3}$ (blue) and the postulated [3,10] $\text{Li}_2\text{B}_{12}\text{H}_{12}$ crystal structures of $\text{C}2/m$ (green) and $\text{P}2_1/n$ symmetry (red), and the results of an isolated anion (gold) calculation. Error bars represent $\pm 1\sigma$. (N.B.: 1 meV = 8.065 cm^{-1} .) (For interpretation of the references to color in this figure legend, the reader is referred to the web version of the article.)

a lack of long-range order for the former, the spectral features of both are essentially the same and agree well with the simulated spectrum for the $\text{Pa}\bar{3}$ structure solved from powder XRD data [16]. Since NVS is a more local probe than XRD, this similarity in spectral features suggests that the amorphous $\text{Li}_2\text{B}_{12}\text{H}_{12}$ possesses short-range-ordered arrangements very similar to the arrangements in the long-range ordered crystalline sample. The observed spectra are also compared with spectra simulated from the results of DFT calculations for previously suggested crystal structures of $\text{C}2/m$ and $\text{P}2_1/n$ symmetries [3,10] as well as for the isolated anion. There are marked differences in the calculated spectral features for these different crystal structures and the isolated anion. It is clear that the simulated spectrum of the experimentally observed $\text{Pa}\bar{3}$ structure is in best agreement with the neutron vibrational spectrum. These results demonstrate that the vibrational spectra for these

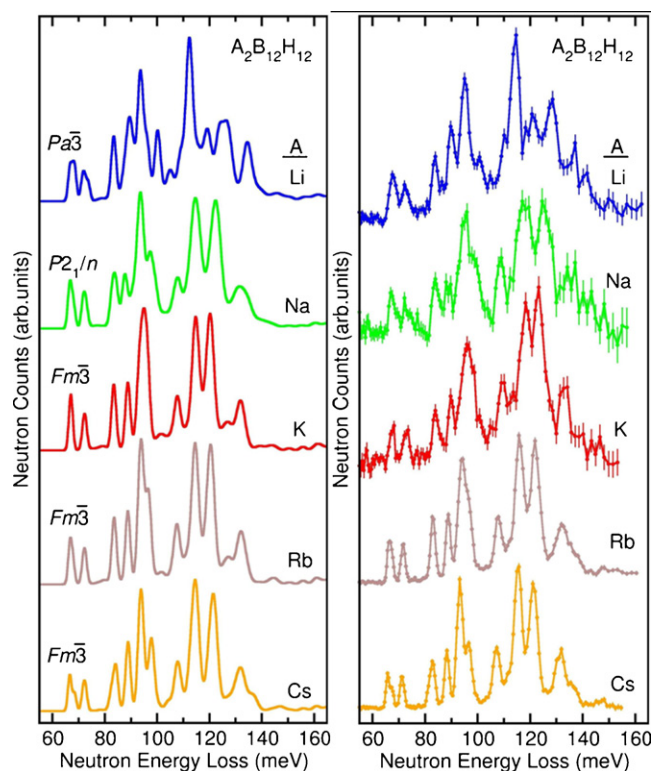


Fig. 2. Alkali metal $B_{12}H_{12}$ NVS spectra. The simulated (left) and experimental (right) neutron vibrational spectra are compared for (from top to bottom): $Li_2B_{12}H_{12}$ (blue), $Na_2B_{12}H_{12}$ (green), $K_2B_{12}H_{12}$ (red), $Rb_2B_{12}H_{12}$ (brown) and $Cs_2B_{12}H_{12}$ (gold). The simulated spectra are the result of an optimized geometry DFT calculation for the experimentally determined crystal structure with the space group indicated. (For interpretation of the references to color in this figure legend, the reader is referred to the web version of the article.)

types of compounds are indeed sensitive to crystal structure, and that it is possible to corroborate the presence of a particular structural arrangement by using NVS in conjunction with DFT phonon calculations.

The observed neutron vibrational spectra of the other alkali metal dodecahydro-*closo*-dodecaborates and the spectra simulated from DFT phonon calculations of the optimized XRD structures [16–18] are compared in Fig. 2. The agreement between the observed and calculated neutron vibrational spectra is strikingly good. It has been reported by some of us [17] that the alkali metal series of $B_{12}H_{12}^{2-}$ compounds is one in which the arrangement of cations about the $B_{12}H_{12}^{2-}$ anion changes with cationic radius. The K^+ , Rb^+ , and Cs^+ cations are in a cubic arrangement about the $B_{12}H_{12}$ icosahedron, the Li^+ is in an octahedral configuration, and the Na^+ is distorted from either arrangement. Similarly, the neutron vibrational spectra differ with space group. The compounds with the larger cations, all of which form cubic crystal structures with $Fm\bar{3}$ symmetry, exhibit similar spectra. The spectrum for the compound with a smaller cationic radius, $Na_2B_{12}H_{12}$ (with $P2_1/n$ symmetry), deviates somewhat from these, while that with the smallest cationic radius, $Li_2B_{12}H_{12}$ (with $Pa\bar{3}$ symmetry), is distinctly different. The arrangements of the alkali counter-ions about the $B_{12}H_{12}^{2-}$ anion for each space group are illustrated in Fig. 3.

Two spectral features seem most sensitive to environment for the alkali series, and are in fact absent from the spectrum of the isolated $B_{12}H_{12}^{2-}$ anion. One is found at 123–128 meV, depending on counter-ion, appearing as a doublet paired with a less environment-dependent peak at 115–118 meV. The higher energy peak shifts with crystal structure and may split into two or more peaks in the lithium spectrum. This spectral region includes hydrogen wagging

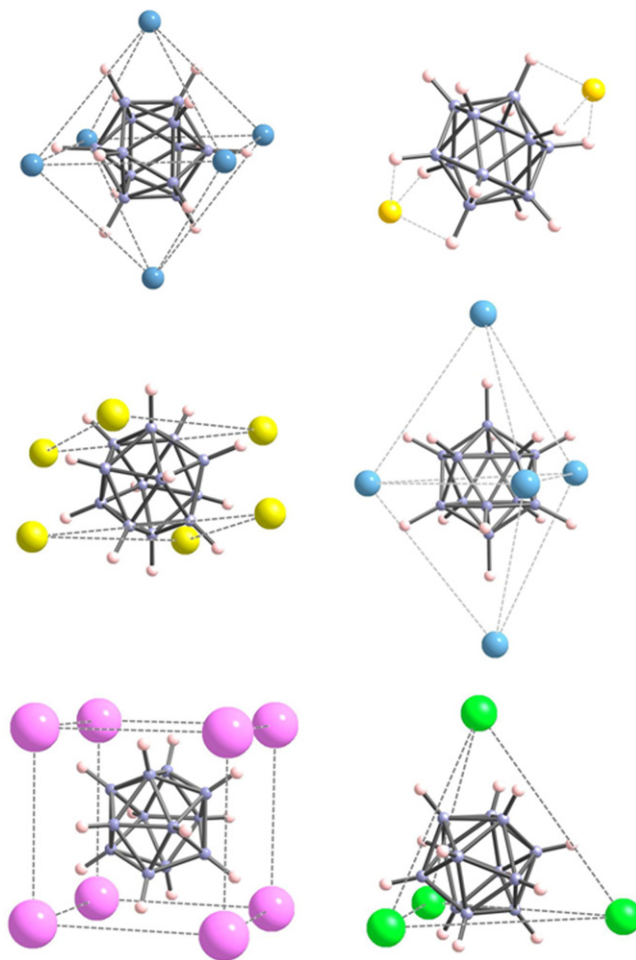


Fig. 3. $B_{12}H_{12}$ polyhedra in different crystal environments. The left column shows the $B_{12}H_{12}^{2-}$ anion as found in the Li ($Pa\bar{3}$, top left), Na ($P2_1/n$, center left) and Cs ($Fm\bar{3}$, bottom left) counter-ion crystal environments. The right column shows the $B_{12}H_{12}^{2-}$ anion as predicted for the Mg ($C2/m$, top right) and found experimentally for the Ca ($C2/c$, center right), and Sr ($P31c$, bottom right) counter-ion crystal environments.

motions which may be influenced by the sterics and symmetry of the surrounding crystalline environment. Another feature sensitive to the crystal environment is found between 95 meV and 100 meV. It appears as a doublet in which two (or more) peaks vary in relative intensity with counter-ion.

Within a given symmetry group, the differences between spectra are minor for different counter-ions. The spectra of the cubic K , Rb , and Cs dodecahydro-*closo*-dodecaborates display only subtle differences, manifested as small (1 meV) frequency shifts and slight variations in peak widths. The variations in peak widths are in part attributed to sample crystallinity, which varied from sample to sample as evidenced by XRD.

A solid-state ^{11}B and 1H NMR spectroscopic study on $A_2B_{12}H_{12}$ (where $A=K, Rb, \text{ and } Cs$) [19] found that the activation energy for hydrogen rotational reorientation decreases as the cationic radius increases, with a corresponding increase in the crystal lattice parameters. As the cationic radius decreases, so does the A–H distance. Hence, the smaller cations impose larger steric forces on the $B_{12}H_{12}^{2-}$ anion, which, as the NMR study concludes, hinders the hydrogen motion. The implication for the current study is that the molecular vibrations will deviate most from those of the isolated molecule for crystals with the smallest cations: *i.e.*, Li^+ and Na^+ . For example, we find that the vibration at 122–123 meV in the cubic crystal (K^+ , Rb^+ , Cs^+) shifts to 125 meV in the $P2_1/n$

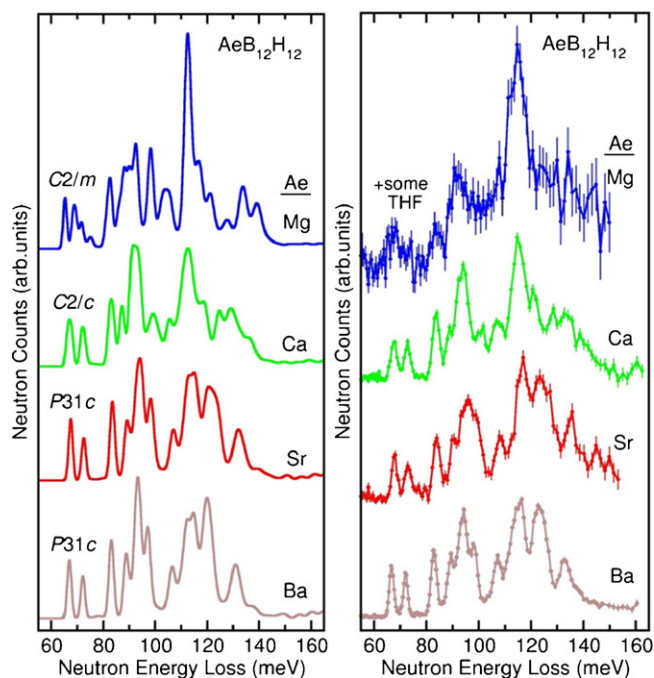


Fig. 4. Alkaline-earth metal $B_{12}H_{12}$ NVS spectra. Simulated (left) and experimental (right) neutron vibrational spectra for (top to bottom): $MgB_{12}H_{12}$ (blue), $CaB_{12}H_{12}$ (green), $SrB_{12}H_{12}$ (red), and $BaB_{12}H_{12}$ (brown). The simulated spectra are the result of an optimized geometry DFT calculation for the experimentally determined crystal structure (with the exception of the $MgB_{12}H_{12}$ which is a predicted structure) with the space group indicated. (For interpretation of the references to color in this figure legend, the reader is referred to the web version of the article.)

($Na_2B_{12}H_{12}$) compound and 129 meV in the $Pa\bar{3}$ ($Li_2B_{12}H_{12}$) compound.

In addition to the alkali metal compounds, the neutron vibrational spectra of the alkaline-earth metal compounds $MgB_{12}H_{12}$, $CaB_{12}H_{12}$, $SrB_{12}H_{12}$, and $BaB_{12}H_{12}$ were measured and compared with the simulated spectra from DFT calculations, as shown in Fig. 4. As mentioned earlier, the $MgB_{12}H_{12}$ sample retained some THF solvent molecules and was XRD-amorphous. The optimized geometries of the latter three were obtained by powder XRD [9,20]. The geometry for solvent-free $MgB_{12}H_{12}$ came from the theoretically derived structure of Ozolins et al. [10].

As with the alkali metal compounds, the structures of the alkaline-earth metal compounds are largely governed by the size of the counter-ion, and the vibrational spectra are very similar for those with isomorphic structures, i.e., $SrB_{12}H_{12}$ and $BaB_{12}H_{12}$, both possessing $P31c$ symmetry [20]. The Sr^{2+} and Ba^{2+} cations are arranged tetrahedrally about the $B_{12}H_{12}^{2-}$ anion while the Ca^{2+} cations are in an octahedral arrangement, as demonstrated in Fig. 3. The $SrB_{12}H_{12}$ and $BaB_{12}H_{12}$ differ from the $CaB_{12}H_{12}$ ($C2/c$) and $MgB_{12}H_{12}$ ($C2/m$) spectra primarily in the intensity and width of the observed peaks at 98 meV and 125 meV. These features are sharper and shifted in the $CaB_{12}H_{12}$ spectrum, presumably due to a density of states with less mode dispersion and a different crystal environment compared with that of $SrB_{12}H_{12}$ and $BaB_{12}H_{12}$. Those peaks may be similarly weak or completely absent from the observed $MgB_{12}H_{12}$ spectrum.

The inability to completely desolvate the $MgB_{12}H_{12}$ compound precludes a definitive comparison of the observed spectrum with that for the theoretically derived anhydrous structure. Clearly the THF is perturbing somewhat the vibrational density of states for $MgB_{12}H_{12}$. Yet, the observed spectrum of this amorphous sample does possess some similarities with the simulated spectrum, especially in the region near 115 meV, where both indicate an unusually intense scattering band compared to the other dodecahydro-closododecaborate compounds. This may indeed reflect the propensity of $MgB_{12}H_{12}$ to crystallize in the same structure as predicted, although this can only be corroborated by the measurement of a fully anhydrous sample. To date, it has not been possible to remove solvent molecules from $MgB_{12}H_{12}$ completely without partial reaction with the $B_{12}H_{12}^{2-}$ anions. Work is ongoing to find a solution to this problem.

5. Conclusions

A neutron vibrational spectroscopy study of $A_2B_{12}H_{12}$ and $AeB_{12}H_{12}$ compounds indicates that the internal vibrations of the $B_{12}H_{12}^{2-}$ icosahedral anions are sensitive to symmetry-dependent interactions with their crystal surroundings, and spectral details were found to differ considerably with structure. These results confirm that the combination of NVS and DFT phonon calculations can help validate possible structural symmetries in these types of materials, even when the materials appear amorphous and/or are part of a mixture of other reaction products.

Acknowledgements

The authors thank Drs. Craig M. Brown and John J. Rush for useful discussions. The authors express special thanks to Dr. Satish S. Jal- isatgi for generously providing the $Li_2B_{12}H_{12}$ sample. This work was supported by the DOE through Award Nos. DE-AL-01-05EE11104 and DE-AC04-94AL8500.

References

- [1] S.-J. Hwang, et al., J. Phys. Chem. C 112 (2008) 3164.
- [2] L. Mosegaard, et al., J. Alloys Compd. 446–447 (2007) 301.
- [3] N. Ohba, et al., Phys. Rev. B 74 (2006) 075110.
- [4] S.-I. Orimo, et al., Appl. Phys. Lett. 89 (2006) 021920.
- [5] G.L. Soloveichik, et al., Int. J. Hydrogen Energy 34 (2009) 916.
- [6] H.-W. Li, et al., Nanotechnology 20 (2009) 204013.
- [7] R.J. Newhouse, V. Stavila, S.-J. Hwang, L.E. Klebanoff, J.Z. Zhang, J. Phys. Chem. C 114 (2010) 5224.
- [8] O. Friedrichs, A. Remhof, S.-J. Hwang, A. Züttel, Chem. Mater. 22 (2010) 3265.
- [9] V. Stavila, et al., J. Solid State Chem. 183 (2010) 1133.
- [10] V. Ozolins, E.H. Majzoub, C. Wolverton, JACS 131 (2009) 230.
- [11] L.A. Leites, et al., Spectrochim. Acta 38 A (1982) 1047.
- [12] D.G. Allis, B.S. Hudson, J. Phys. Chem. A 110 (2006) 3744.
- [13] T.J. Udovic, et al., Nucl. Instrum. Methods A 588 (2008) 406.
- [14] P. Giannozzi, et al., J. Phys.: Condens. Matter 21 (2009) 395502.
- [15] G. Kresse, J. Furthmüller, J. Hafner, Europhys. Lett. 32 (1995) 729.
- [16] J.-H. Her, et al., Inorg. Chem. 47 (2008) 9757.
- [17] J.-H. Her, W. Zhou, V. Stavila, C.M. Brown, T.J. Udovic, J. Phys. Chem. C 113 (2009) 11187.
- [18] I. Tiritiris, T. Schleid, Z. Anorg. All. Chem. 629 (2003) 1390.
- [19] I. Tiritiris, T. Schleid, K. Müller, Appl. Magn. Reson. 32 (2007) 459.
- [20] J.-H. Her, et al., in preparation, 2010.